

---

This is an electronic reprint of the original article.  
This reprint may differ from the original in pagination and typographic detail.

Author(s): Hakala, M. & Puska, M. J. & Nieminen, Risto M.

Title: Native defects and self-diffusion in GaSb

Year: 2002

Version: Final published version

**Please cite the original version:**

Hakala, M. & Puska, M. J. & Nieminen, Risto M. 2002. Native defects and self-diffusion in GaSb. *Journal of Applied Physics*. Volume 91, Issue 8. 4988-4994. ISSN 0021-8979 (printed). DOI: 10.1063/1.1462844.

Rights: © 2002 American Institute of Physics. This is the accepted version of the following article: Hakala, M. & Puska, M. J. & Nieminen, Risto M. 2002. Native defects and self-diffusion in GaSb. *Journal of Applied Physics*. Volume 91, Issue 8. 4988-4994. ISSN 0021-8979 (printed). DOI: 10.1063/1.1462844, which has been published in final form at <http://scitation.aip.org/content/aip/journal/jap/91/8/10.1063/1.1462844>.

---

All material supplied via Aaltodoc is protected by copyright and other intellectual property rights, and duplication or sale of all or part of any of the repository collections is not permitted, except that material may be duplicated by you for your research use or educational purposes in electronic or print form. You must obtain permission for any other use. Electronic or print copies may not be offered, whether for sale or otherwise to anyone who is not an authorised user.

## Native defects and self-diffusion in GaSb

M. Hakala, M. J. Puska, and R. M. Nieminen

Citation: *Journal of Applied Physics* **91**, 4988 (2002); doi: 10.1063/1.1462844

View online: <http://dx.doi.org/10.1063/1.1462844>

View Table of Contents: <http://scitation.aip.org/content/aip/journal/jap/91/8?ver=pdfcov>

Published by the [AIP Publishing](#)

---

### Articles you may be interested in

#### [Native point defects in GaSb](#)

*J. Appl. Phys.* **116**, 143508 (2014); 10.1063/1.4898082

#### [Point defect balance in epitaxial GaSb](#)

*Appl. Phys. Lett.* **105**, 082113 (2014); 10.1063/1.4894473

#### [Antisites and anisotropic diffusion in GaAs and GaSb](#)

*Appl. Phys. Lett.* **103**, 142107 (2013); 10.1063/1.4824126

#### [Concentration of intrinsic defects and self-diffusion in GaSb](#)

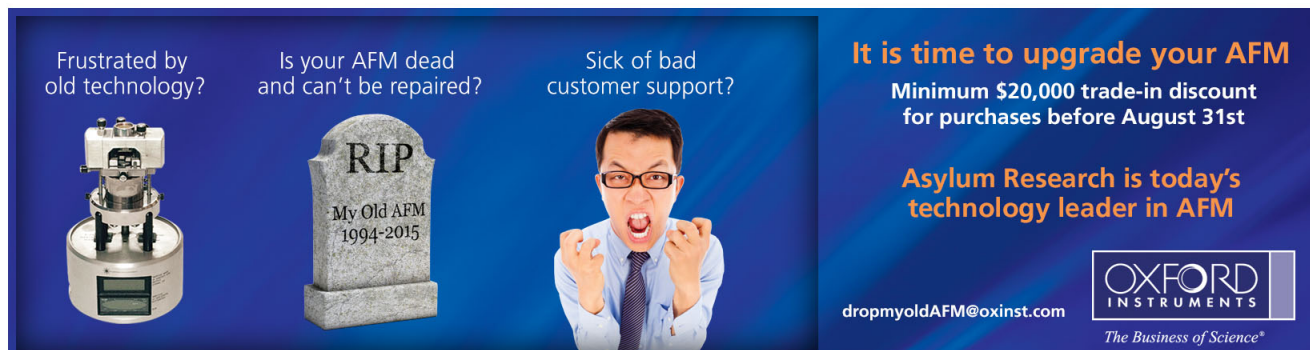
*J. Appl. Phys.* **104**, 093714 (2008); 10.1063/1.3010300

#### [Self-diffusion in 69 Ga 121 Sb/ 71 Ga 123 Sb isotope heterostructures](#)

*J. Appl. Phys.* **89**, 5393 (2001); 10.1063/1.1363683

---

Frustrated by old technology?      Is your AFM dead and can't be repaired?      Sick of bad customer support?



**It is time to upgrade your AFM**  
Minimum \$20,000 trade-in discount for purchases before August 31st

**Asylum Research is today's technology leader in AFM**

[dropmyoldAFM@oxinst.com](mailto:dropmyoldAFM@oxinst.com)

**OXFORD INSTRUMENTS**  
The Business of Science®

## Native defects and self-diffusion in GaSb

M. Hakala,<sup>a)</sup> M. J. Puska, and R. M. Nieminen

Laboratory of Physics, Helsinki University of Technology, P.O. Box 1100, FIN-02015 HUT, Finland

(Received 19 July 2001; accepted for publication 29 January 2002)

The native defects in GaSb have been studied with first-principles total-energy calculations. We report the structures and the formation energies of the stable defects and estimate the defect concentrations under different growth conditions. The most important native defect is the  $\text{Ga}_{\text{Sb}}$  antisite, which acts as an acceptor. The other important defects are the acceptor-type Ga vacancy and the donor-type Ga interstitial. The Sb vacancies and interstitials are found to have much higher formation energies. A metastable state is observed for the  $\text{Sb}_{\text{Ga}}$  antisite. The significantly larger concentrations of the Ga vacancies and interstitials compared to the corresponding Sb defects is in accordance with the asymmetric self-diffusion behavior in GaSb. The data supports the next-nearest-neighbor model for the self-diffusion, in which the migration occurs independently in the different sublattices. Self-diffusion is dominated by moving Ga atoms. © 2002 American Institute of Physics. [DOI: 10.1063/1.1462844]

### I. INTRODUCTION

Gallium antimonide is a technologically interesting material due to its applications to high speed electronic and long wavelength photonic devices (for a review, see Ref. 1). The narrow, direct band gap of 0.73 eV (at 300 K) of GaSb enables its use in the fabrication of infrared detectors and sources. GaSb can be lattice matched with ternary and quaternary III-V compounds to form a substrate material for various optical communication devices, which operate in the 2–4  $\mu\text{m}$  regime. Furthermore, GaSb has a high electron mobility and saturation velocity, which can be utilized in high electron mobility transistors. In these devices band offsets of GaSb with similar compounds can be used to create the conducting two-dimensional electron gas. Interesting basic problems in GaSb are the origin of its residual acceptor concentration and the recently observed strongly asymmetric self-diffusion.<sup>2,3</sup> GaSb is always *p* type irrespective of growth techniques and conditions.<sup>1</sup> The typical residual acceptor concentration is  $\sim 10^{17} \text{ cm}^{-3}$ , and the acceptors are associated with native Ga vacancies and antisite defects.<sup>1</sup> Nonstoichiometric growth conditions have been used to reduce the acceptor concentration and increase the hole mobility.<sup>4,5</sup> Self-diffusion is related to material degradation, and it is strongly correlated to lattice defects and the diffusion of impurities.

The recent experiments by Bracht *et al.*<sup>2,3</sup> have demonstrated that Ga diffuses several orders of magnitude faster than Sb. The authors have proposed a model according to which the diffusion takes place independently in the different sublattices, which points to a next-nearest-neighbor diffusion mechanism. According to the model Ga diffuses via vacancies, whereas Sb diffuses via interstitials. The large difference in the diffusion coefficients derives from a significant concentration difference between the Ga vacancies and the Sb interstitials. The concentrations are explained to be

strongly affected by amphoteric transformations, which increase the number of Ga vacancies and reduce the number of Sb interstitials. Since the defects may possess several charge states, the energetics of amphoteric reactions is proposed to depend on the Fermi level position.

Electronic structure calculations have been extensively used in the analysis of properties of native defects in III-V materials. GaAs is the most studied material, and to a large extent the results can be generalized to other III-V materials.<sup>6</sup> The defects with intrinsic metastabilities have attracted particular interest in III-V materials.<sup>7</sup> For example, the detection of a defect may depend on whether it is in the stable or the metastable configuration. It is interesting to see whether this structural property is found in GaSb. For GaSb, there are few electronic structure calculations available. The existing data is usually calculated as a part of a series where the chemical trends of III-V materials have been analyzed. Kühn *et al.*<sup>8</sup> have studied vacancies and antisite defects using charge-self-consistent empirical tight-binding methods. Xu<sup>9</sup> has studied vacancies with semiempirical tight-binding methods, while Talwar and Ting<sup>10</sup> have studied vacancies and antisites using Green's function tight-binding methods. Puska<sup>11</sup> has studied vacancies and antisites with linear-muffin-tin-orbital Green's function methods. All the above-mentioned studies are for ideal atomic structures.

In this work we have studied the electronic structures and the formation energies of native defects in GaSb with *ab initio* methods. The calculations have been performed for fully relaxed vacancies, interstitials, and antisite defects. We show that the defects behave to a large extent in a similar way to those in GaAs. We calculate the defect concentrations at typical growth temperatures. We show that the residual acceptor is the gallium antisite defect and estimate the effect of growth conditions on the residual hole concentration. We study the model by Bracht *et al.*<sup>2,3</sup> for the asymmetric self-diffusion, the proposed amphoteric transformations, and comment on the probability of the nearest-neighbor diffusion mechanism.

<sup>a)</sup>Electronic mail: moh@fyslab.hut.fi

The paper is organized as follows. In Sec. II we describe the theoretical methods and the calculation of the defect formation energies and concentrations. In Sec. III we present the results for the atomic and electronic structure of the stable native defects and study the concentrations of the defects, especially those of residual acceptors. In Sec. IV the self-diffusion is discussed in the light of our data. Finally, Sec. V presents the conclusions.

## II. METHODS

The structures and the total energies of the native defects are calculated within the density-functional theory<sup>12</sup> and the local-density approximation (LDA).<sup>13</sup> The plane-wave pseudopotential method<sup>14</sup> is used with nonlocal norm-conserving pseudopotentials: for Ga a Hamann type<sup>15</sup> and for Sb a Troullier-Martins type.<sup>16</sup> The  $3d$  and  $4d$  electrons of Ga and Sb, respectively, are included in the core. The nonlinear core-valence exchange-correlation scheme<sup>17</sup> is used for both elements. With these pseudopotentials the theoretical (experimental<sup>1</sup>) lattice constant is  $6.01 \text{ \AA}$  ( $6.10 \text{ \AA}$ ), the bulk modulus  $0.548 \text{ Mbar}$  ( $0.563 \text{ Mbar}$ ) and the band gap is  $0.31 \text{ eV}$  ( $0.82 \text{ eV}$  at  $0 \text{ K}$ ). The band gap underestimation is typical for the LDA calculations.

We have used a 64-atom supercell with the optimized lattice constant and a  $\mathbf{k}$ -point sampling proposed by Makov *et al.*<sup>18</sup> The sampling consists of points  $(0, 0, 0)$  and  $(\frac{1}{2}, \frac{1}{2}, \frac{1}{2})$  in units of  $(2\pi/a)$ , where  $a$  is the lattice constant of the supercell. This sampling and supercell size have been found to be a good approximation for the formation energies for point defects in semiconductors,<sup>19</sup> tending to minimize the interactions between a defect and its periodic replica.<sup>18</sup> The approximation may lead to a slight indefiniteness in the point symmetry group of the defects.<sup>19</sup> We use a 22-Ry kinetic energy cutoff, which leads to well-converged atomic structures. Our starting configurations are the ideal structures for vacancies, antisites, and interstitials. For interstitials we use as starting configurations the two inequivalent tetrahedral sites and the hexagonal site. A small random component is added to the initial atomic coordinates to break the high symmetry of the initial configuration. The ions are allowed to relax with no symmetry restrictions following the Hellmann–Feynman forces until the largest force component on any atom is less than  $5 \text{ meV/\AA}$ .

The formation energies of the defects are calculated following the formalism used by Zhang and Northrup.<sup>20</sup> The formation energy of a defect is written as

$$E_f = E_D + q(\mu_e + E_v) - n_{\text{Ga}}\mu_{\text{Ga}} - n_{\text{Sb}}\mu_{\text{Sb}}, \quad (1)$$

where  $E_D$  is the total energy of the supercell containing the defect in question,  $q$  the charge (electrons or holes) transferred to the defect from a reservoir,  $\mu_e$  the chemical potential of the reservoir, and  $E_v$  the valence band maximum (VBM).  $\mu_e$  corresponds to the Fermi level calculated from the VBM. To account for the Coulomb interaction between a charged defect and its periodic replicas, we have added a Madelung-type monopole correction term to  $E_D$ .<sup>21</sup>  $n_{\text{Ga}}$  and  $n_{\text{Sb}}$  are the number of each element in the supercell. The atomic chemical potentials obtain values below their bulk

precipitates:  $\mu_{\text{Ga}} \leq \mu_{\text{Ga}(\text{bulk})}$  and  $\mu_{\text{Sb}} \leq \mu_{\text{Sb}(\text{bulk})}$ . It is also required that the sum of the chemical potentials equals the chemical potential per atom pair in the bulk compound:  $\mu_{\text{Ga}} + \mu_{\text{Sb}} = \mu_{\text{GaSb}}$ .

Equation (1) can be rewritten as

$$E_f = E'_D + q\mu_e - \frac{1}{2}(n_{\text{Ga}} - n_{\text{Sb}})\Delta\mu, \quad (2)$$

where

$$E'_D = E_D - \frac{1}{2}(n_{\text{Ga}} + n_{\text{Sb}})\mu_{\text{GaAs}} - \frac{1}{2}(n_{\text{Ga}} - n_{\text{Sb}})(\mu_{\text{Ga}(\text{bulk})} - \mu_{\text{Sb}(\text{bulk})}) + qE_v \quad (3)$$

and

$$\Delta\mu = (\mu_{\text{Ga}} - \mu_{\text{Sb}}) - (\mu_{\text{Ga}(\text{bulk})} - \mu_{\text{Sb}(\text{bulk})}). \quad (4)$$

$\mu_{\text{Ga}(\text{bulk})}$  and  $\mu_{\text{Sb}(\text{bulk})}$  are calculated from their elemental bulk phases. The electron chemical potential  $\mu_e$  is allowed to vary between zero and the experimental band gap value,  $0 \leq \mu_e \leq E_g$ . The limits for the chemical potential  $\Delta\mu$  are given by the heat of formation  $\Delta H$  of GaSb,  $-\Delta H \leq \Delta\mu \leq \Delta H$ . The values closer to  $-\Delta H$  correspond to Sb-rich growth conditions and values closer to  $\Delta H$  to Ga-rich growth conditions. If  $\Delta\mu$  were defined using the chemical potentials of other than the elemental solid phases, i.e., those of the elemental molecular gases, the range of variation of  $\Delta\mu$  would increase. We use the experimental value of  $0.43 \text{ eV}$  for  $\Delta H$ .<sup>22</sup> Our calculated theoretical value is  $(-0.1 \pm 0.3) \text{ eV}$ ; the discrepancy may be explained by the shortcomings of the LDA calculation, since  $\Delta H$  requires a very accurate calculation of the energy difference between the compound and the elements in bulk phase.

The concentration of a given defect is

$$C_D = z_D N_s \exp(-F_f/k_B T), \quad (5)$$

where  $z_D$  is the number of equivalent configurations for a particular defect per sublattice site,  $N_s$  the density of sublattice sites ( $1.7 \times 10^{22} \text{ cm}^{-3}$ ),  $F_f$  the free energy of defect formation,  $k_B$  the Boltzmann constant, and  $T$  the equilibrium sample temperature. In our calculations we have omitted the entropy part in  $F_f$  and use only the formation energies when estimating the concentrations. The entropy differences can be of the order of  $3k_B$ ,<sup>6</sup> which corresponds to internal energies  $\sim 0.2 \text{ eV}$  in the temperature range of  $400$  to  $500 \text{ }^\circ\text{C}$ . The charge neutrality condition is used to define the Fermi level position.<sup>20</sup> Thermally created charge carriers in the valence and the conduction bands are included in the self-consistent determination of the Fermi level. The effective densities of states of the valence and conduction bands are calculated from the effective masses of electrons and holes.<sup>1</sup> In showing the relative defect concentrations we use the temperature  $450 \text{ }^\circ\text{C}$ , which corresponds to the growth temperature of the molecular beam epitaxy (MBE) method used in the experiments by Bracht *et al.*<sup>2,3</sup>

The additional error sources in the formation energy are as follows. The plane-wave convergence error was found to be  $\sim 0.05 \text{ eV}$  and the convergence error in the atomic chemical potentials  $\sim 0.25 \text{ eV}$ . The used supercell size and the  $\mathbf{k}$ -point sampling may also induce errors in the formation



TABLE I. Charge states, point symmetry groups, and formation energies of the native defects in GaSb. The point symmetries are deduced from the converged positions of the ions neighboring the defect.

| Defect                                      | Symmetry <sup>a</sup> | $E_f$ (eV)                       |
|---|-----------------------|----------------------------------|
| $V_{\text{Ga}}^{3-}$                        | $T_d$                 | $2.62 + (1/2)\Delta\mu - 3\mu_e$ |
| $V_{\text{Ga}}^{2-}$                        | $\sim T_d$            | $2.07 + (1/2)\Delta\mu - 2\mu_e$ |
| $V_{\text{Ga}}^{1-}$                        | $\sim D_{2d}$         | $1.76 + (1/2)\Delta\mu - \mu_e$  |
| $V_{\text{Sb}}^{1+}$                        | $\sim T_d$            | $1.93 - (1/2)\Delta\mu + \mu_e$  |
| $V_{\text{Sb}}^0$                           | $\sim C_{2v}$         | $1.11 - (1/2)\Delta\mu$          |
| $V_{\text{Sb}}^{1-}$                        | $\sim D_{2d}$         | $2.31 - (1/2)\Delta\mu - \mu_e$  |
| $\text{Ga}_{\text{Sb}}^{2-}$                | $T_d$                 | $1.43 - \Delta\mu - 2\mu_e$      |
| $\text{Ga}_{\text{Sb}}^{1-}$                | $\sim T_d$            | $1.17 - \Delta\mu - \mu_e$       |
| $\text{Ga}_{\text{Sb}}^0$                   | $\sim C_{3v}$         | $1.13 - \Delta\mu$               |
| $\text{Sb}_{\text{Ga}}^0$                   | $T_d$                 | $1.33 + \Delta\mu$               |
| $\text{Ga}_i^{1+}(T_c)$                     | $T_d$                 | $0.77 - (1/2)\Delta\mu + \mu_e$  |
| $\text{Sb}_i^{3+}(T_a)$                     | $T_d$                 | $3.77 + (1/2)\Delta\mu + 3\mu_e$ |
| $\text{Sb}_i^{1+}(H)$                       | $C_{3v}$              | $2.80 + (1/2)\Delta\mu + \mu_e$  |
| $\text{Sb}_i^{1+}(T_c)$                     | $\sim D_{2d}$         | $2.96 + (1/2)\Delta\mu + \mu_e$  |
| $(V_{\text{Ga}}\text{Ga}_{\text{Sb}})^{3-}$ | $C_{3v}$              | $2.70 - (1/2)\Delta\mu - 3\mu_e$ |
| $(V_{\text{Ga}}\text{Ga}_{\text{Sb}})^{2-}$ | $\sim C_{3v}$         | $2.18 - (1/2)\Delta\mu - 2\mu_e$ |
| $(V_{\text{Ga}}\text{Ga}_{\text{Sb}})^{1-}$ | $\sim C_{3v}$         | $1.90 - (1/2)\Delta\mu - \mu_e$  |
| $(V_{\text{Sb}}\text{Sb}_{\text{Ga}})^{1+}$ | $C_{1h}$              | $2.35 + (1/2)\Delta\mu + \mu_e$  |
| $(V_{\text{Ga}}\text{Sb}_i)^0$              | $C_{3v}$              | $1.56 + \Delta\mu$               |

<sup>a</sup>Reference 23.

energy. We assume that these deviations are not critical for the formation energy and concentration differences.

Finally, the ionization level ( $q/q'$ ) of a defect is defined as the position of the Fermi level when two given charge states have the same total energy:

$$E_D^q + Q[E_v^q + \mu_e^{(q/q')}] = E_D^{q'} + q'[E_v^{q'} + \mu_e^{(q/q')}] \quad (6)$$

One should note that the used monopole correction (see above) affects the level positions strongly for the higher charge states. For example, the  $(3-/2-)$  level is corrected by 0.6 eV. As the higher-order terms in the expansion for the electrostatic energy decrease the magnitude of the correction, the monopole shifts provide an upper bound.

### III. NATIVE DEFECTS

#### A. Structures and energies

The charge states, the symmetries and the formation energies for the native defects in GaSb are presented in Table I. The ionization levels are given in Table II. In general, the electronic structure of the vacancies, antisites and interstitials

TABLE II. Ionization levels for the stable native defects.

| Defect                               | Ionization level | Energy (eV)  |
|--------------------------------------|------------------|--------------|
| $\text{Ga}_{\text{Sb}}$              | (0/1-)           | $E_v + 0.04$ |
|                                      | (1-/2-)          | $E_v + 0.26$ |
| $V_{\text{Ga}}$                      | (0/1-)           | $E_v + 0.00$ |
|                                      | (1-/2-)          | $E_v + 0.31$ |
|                                      | (2-/3-)          | $E_v + 0.55$ |
| $V_{\text{Sb}}$                      | (1+/0)           | $E_v + 0.18$ |
|                                      | (0/1-)           | $E_v + 0.20$ |
| $V_{\text{Ga}}\text{Ga}_{\text{Sb}}$ | (1-/2-)          | $E_v + 0.28$ |
|                                      | (2-/3-)          | $E_v + 0.52$ |

is in qualitative agreement with the other III-V compounds.<sup>6</sup> The formation energy is affected by the Fermi level position due to the fact that the defects can exist in different charge states. Among the vacancy defects,  $V_{\text{Ga}}$  acts as a triple acceptor: 1–3 electrons can be added to the defect with a positive extra energy per each added electron. The electrons are distributed to the four Sb dangling bonds. In the  $(3-)$  charge state the defect preserves the  $T_d$  symmetry with an inward relaxation (12%) of the nearest neighbor atoms of the vacancy. For the  $(2-)$  and  $(1-)$  charge states there is an additional symmetry-breaking distortion, which indicates that the partially occupied  $t_2$  level is split.  $V_{\text{Sb}}$  can be found with the charge states  $(1+)$ ,  $(0)$  and  $(1-)$ . In the  $(1+)$  charge state the symmetry group is  $\sim T_d$  (Ref. 23) with an inward relaxation of 5%. The smaller relaxation indicates that the accompanying energy release is smaller than for  $V_{\text{Ga}}$ . The  $(1+/0)$  and  $(0/1-)$  levels were found close to each other at  $\sim 0.2$  eV. In the  $(0)$  charge states the symmetry of  $V_{\text{Sb}}$  is lowered to  $C_{2v}$  as a gap state is occupied. Double occupancy of the gap level leads to a very strong inwards relaxation ( $\sim 20\%$ ) with the symmetry of  $D_{2d}$ . The strong relaxation is very similar to that found for the negatively charged  $V_{\text{As}}$  in GaAs.<sup>24</sup> The systematic feature in the present calculation is that the relaxation is always towards the vacancy. In GaAs, an outward relaxation for  $V_{\text{As}}$  [for the  $(1+)$  and  $(0)$  charge states] has been reported.<sup>24</sup>

The antisite  $\text{Ga}_{\text{Sb}}$  is stable in the  $(0)$ ,  $(1-)$ , and  $(2-)$  charge states and acts as a double acceptor. In the  $(2-)$  charge states the bonding  $t_2$  level is fully occupied and the defect preserves the  $T_d$  symmetry relaxing inwards (9%). The transition levels are in the lower half of the band gap. The additional symmetry-breaking distortions for the  $(1-)$  and  $(0)$  charge states indicate that the partially occupied  $t_2$  level is split. The double acceptor behavior is similar to the Ga antisite in GaAs.<sup>20,25</sup> For the  $\text{Sb}_{\text{Ga}}$  antisite in the  $(0)$  charge state two electrons occupy the antibonding  $a_1$  state. The  $T_d$  symmetry is preserved and the defect relaxes outwards (11%). As electrons are removed from the single-particle state the anion–anion distance decreases. The donor levels  $(2+/1+)$  and  $(1+/0)$  as calculated from the total energies are, however, below the VBM. This is a significantly different behavior from the anion antisite defects in GaAs. In GaAs and InP the donor levels of the anion antisites are located at midgap or above.<sup>7</sup>

For the interstitial defects we studied Ga and Sb atoms at the hexagonal ( $H$ ) and the two tetrahedral sites ( $T_a, T_c$ ). At the  $T_a$  ( $T_c$ ) site the defect has four anions (cations) as nearest neighbors. We find that the interstitials stabilize at positive charge states due to the removal of high-energy dangling bond electrons.  $\text{Ga}_i$  is found stable only at the  $T_c$  site at the  $(1+)$  charge state with a rather low formation energy. In fact, the  $T_a$  and  $H$  starting configurations relax to the  $T_c$  configuration. The absence of states in the band gap indicates that the  $a_1$  level is within the valence band and the unoccupied  $t_2$  level in the conduction band.  $\text{Sb}_i$  is found stable at the  $H$  site and both the  $T$  sites. For the  $T_c$  site the stable charge state is  $(1+)$ . (In fact, the point symmetry is lowered to  $D_{2d}$ .) This is the energetically most favored configuration for all Fermi level positions. The small symmetry-breaking distortion sug-

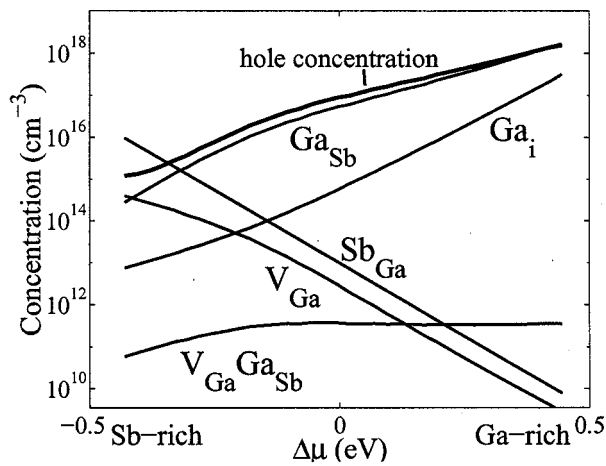


FIG. 1. Native defect concentrations as a function of  $\Delta\mu$  at 450 °C. The residual hole concentration is given by the uppermost thick line. The temperature corresponds to the MBE growth temperature in the experiments by Bracht *et al.* (see Refs. 2, 3). The defect concentrations are given as a sum of the contributions of the different charge states.

gests that the partial occupancy of the  $t_2$  level (close to or within the conduction band) by two electrons leads to the splitting of the level and energy lowering. The interstitial Sb at the  $H$  site has the stable charge state (1+) and an energy of 0.16 eV higher than at the  $T_c^{1+}$  site. Finally, in the  $T_a$  site Sb is stable in the charge state (3+), which preserves the perfect  $T_d$  symmetry. All the  $Sb_i$  defects have a high formation energy compared with  $Ga_i$ , similarly as found for the anion interstitial in GaAs.<sup>20</sup>

The metastability of the anion antisite defects as found for GaAs and InP<sup>7</sup> is also found for GaSb. We find evidence for the transition to the metastable configuration,



which may take place in the neutral charge state. With our set of starting configurations we arrived at the configuration where the Sb atom is displaced 1.66 Å from the substitutional position in the [111] direction towards the  $T_a$  site (see Ref. 7).  $Sb_i$  binds to three nearest neighbor atoms with the bond length of 2.81 Å (cf. 2.88 Å for  $Sb_{Ga}$ ). The energy of the new configuration is 0.23 eV higher than in the antisite configuration. This is similar to that found for several anion antisite defects in GaAs (0.3–0.5 eV).<sup>7</sup> The relative displacement is similar to that found for  $As_{Ga}$  in GaAs.<sup>7</sup>

### B. Concentrations

The  $p$ -type nature of GaSb is naturally explained by the calculations. The concentrations of the native defects and the residual hole concentration at 450 °C are shown in Fig. 1 as a function of the growth conditions. The residual hole concentration originates from  $Ga_{Sb}$ , which is negatively charged [charge state (1–) or (2–) depending on the Fermi level position], and decreases when moving toward Sb-rich conditions. The hole concentration varies between  $10^{15}$  and  $10^{18} \text{ cm}^{-3}$ , which compares fairly well with the experimental observations.<sup>1</sup> Fig. 2 shows the Fermi level position as a function of  $\Delta\mu$  at three temperatures. The temperature range

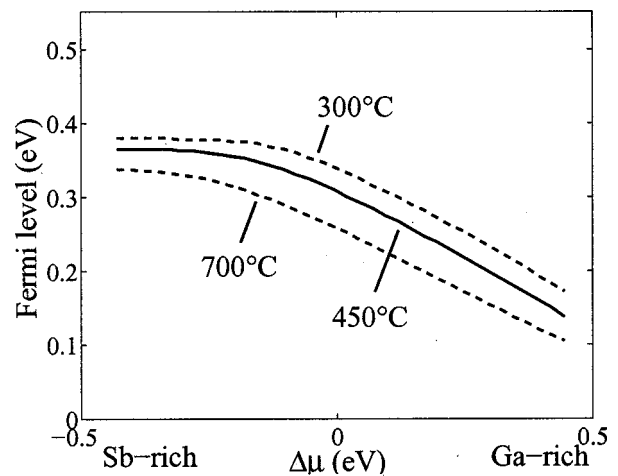


FIG. 2. The Fermi level position as a function of  $\Delta\mu$  for three temperatures.

was chosen to cover roughly the different types of growth temperatures reported in Ref. 1 for bulk and epitaxial growth. When moving toward Ga-rich conditions the increase of the  $Ga_{Sb}$  acceptor concentration is seen to pull the Fermi level downward from its intrinsic value. The other defects are formed less abundantly. For Ga-rich conditions a large concentration is obtained for the positively charged  $Ga_i$ . For Sb-rich conditions the other relevant defects are the negatively charged  $V_{Ga}$  and neutral  $Sb_{Ga}$ . The general trends for the residual hole concentrations are shown in Fig. 3. There is a decrease in the hole concentration when moving from higher to lower temperatures and from Ga-rich to Sb-rich conditions. In comparing GaSb against GaAs one also notes the absence of compensating electrically active defects. In GaAs the anion antisite defect  $As_{Ga}$  with its deep donor levels has been proposed to be responsible for the Fermi level pinning in the middle of the forbidden gap in As-rich conditions.<sup>26</sup> In GaSb the donor levels of the anion antisite defect  $Sb_{Ga}$  are below the VBM and the defect cannot therefore cause compensation.

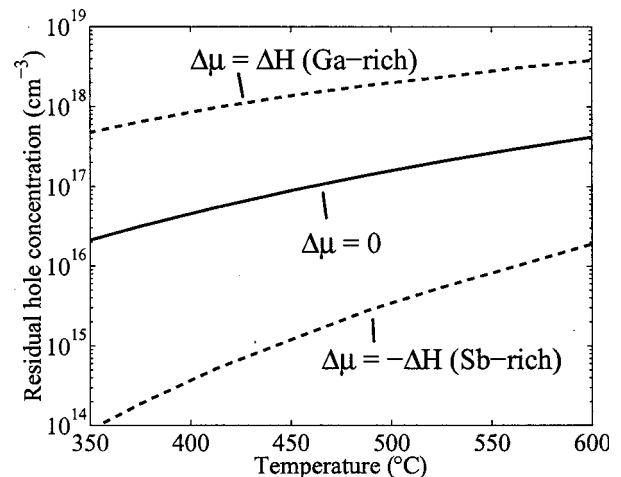


FIG. 3. Residual hole concentration as a function of temperature. The data are shown for the ideal stoichiometry (solid line) and for the Ga- and Sb-rich limits (dashed lines).

Wu and Chen<sup>27</sup> have made a photoluminescence study of high-quality unintentionally doped GaSb layers grown by liquid-phase epitaxy from both Ga- and Sb-rich solutions. They find that transitions of excitons bound to donors and neutral acceptors dominate and that two other bands, A and B, with smaller intensities are related to acceptors. In the sample grown from a Ga-rich solution only the band A is observed, whereas in the Sb-rich case both bands are found with rather similar intensities. Hence, experimental evidence indicates that there are two types of acceptors of which only one is present at Ga-rich conditions, while both are present in similar concentrations in the Sb-rich case. This trend of concentrations correlates with our findings, if we assign the defect responsible for band A to  $V_{\text{Sb}}$ , and that responsible for band B to  $V_{\text{Ga}}$ . Calculated at the appropriate experimental temperatures (530 °C and 635 °C for Ga- and Sb-rich growth types, respectively), the relative concentrations  $[V_{\text{Sb}}]/[V_{\text{Ga}}]$  are  $\sim 10^7$  and  $\sim 1$  for the extreme Ga- and Sb-rich cases, respectively.

#### IV. SELF-DIFFUSION

##### A. Nearest-neighbor diffusion mechanism

The nearest-neighbor diffusion mechanism by vacancies consists of successive atomic movements where a nearest-neighbor atom moves to the vacancy. The relevant reactions for the first steps of the mechanism are written as



In the first reaction  $V_{\text{Ga}}$  can be in different (negative) charge states depending on the Fermi level position (Table I). In contrast, for  $V_{\text{Sb}}\text{Sb}_{\text{Ga}}$  a stable minimum can be found for the (1+) charge state. To the right, the Reaction (8) is *endothermic* and involves electron transfer. We have defined the reaction energy as the formation energy difference between the final and the initial configurations. The reaction energy, calculated for the most stable charge states, increases from 0.6 eV to 1.9 eV as the Fermi level is moved from the VBM to the conduction band minimum (CBM) (we assume the temperature 450 °C, for which the CBM is at  $E_v + 0.55$  eV). The negatively charged starting configurations for  $V_{\text{Sb}}\text{Sb}_{\text{Ga}}$  lead to a direct relaxation to  $V_{\text{Ga}}$ . To the right, the second reaction [Eq. (9)] is, by contrast, *exothermic* for all Fermi level positions.  $V_{\text{Sb}}$  is stable in the (1+), (0), and (1-) charge states, whereas  $V_{\text{Ga}}\text{Ga}_{\text{Sb}}$  can be found in several negative charge states as shown in Table I. The reaction energy decreases from 0 eV to -0.7 eV as the Fermi level is moved from the VBM to the CBM, and this reaction also involves electron transfer.

Qualitatively the Reaction (8) is similar to that found for GaAs by Bockstedte and Scheffler,<sup>28</sup> although in GaAs higher values are found for the reaction energy. For GaAs, for which the diffusion experiments are typically performed in *n*-type or intrinsic material, these authors considered the nearest-neighbor hops irrelevant due to the instability of  $V_{\text{As}}\text{As}_{\text{Ga}}$  in the negative charge state. For GaSb this conclusion may not be valid since the diffusion experiments have

been performed for intrinsic and *p*-type material.<sup>2,3</sup> However, the strong asymmetry in the reaction energies for the nearest-neighbor hops suggests that this mechanism may not be effective in GaSb.

##### B. Next-nearest-neighbor diffusion

In the next-nearest-neighbor diffusion mechanism as suggested by Bracht *et al.*<sup>2,3</sup> the Ga and Sb atoms diffuse independently of each other via either vacancies or interstitials. The self-diffusion coefficient can be defined in the Arrhenius form

$$D_{\text{self}} = D_{\text{self}}^0 \exp(-Q_{\text{self}}/k_B T), \quad (10)$$

where  $Q_{\text{self}}$  is the activation energy of diffusion and  $D_{\text{self}}^0$  the pre-exponential factor. The diffusion coefficient for either Ga or Sb can be written with the help of the concentrations of the relevant defects (vacancies and interstitials) mediating the diffusion:

$$D_{\text{self}} = d_V C_V + d_I C_I. \quad (11)$$

Above, the diffusivity  $d_{V,I}$  contains the factors related to migration (entropy contributions and the migration barrier) and  $C_{V,I}$  are the defect concentrations [Eq. (5)]. The other mechanisms, such as the antisite exchange or the collective diffusive mechanisms, have been neglected in these calculations. Diffusion via antisites cannot be ruled out, but has not been investigated in the present work, because our main goal is to investigate the model proposed by Bracht *et al.*<sup>2,3</sup> On the basis of the calculated concentrations we obtain a simple explanation for the large difference in the Ga and the Sb self-diffusion coefficients as found in experiments.<sup>2,3</sup> Fig. 1 shows the Ga vacancy and interstitial concentrations at  $T = 450$  °C; the calculated Sb vacancy concentration is significantly smaller, increasing from  $\sim 10^7$  to  $\sim 10^9$  cm<sup>-3</sup> as one moves from the Sb-rich limit to the Ga-rich limit. The Sb interstitial concentration at this temperature is negligibly small for all values of  $\Delta\mu$ . By assuming that the diffusivities of the vacancies and interstitials of the two sublattices do not differ drastically, the concentration differences in Eq. (11) would qualitatively explain the strongly asymmetric diffusion behavior.

The important point in our data is that the Ga interstitial concentration is significantly higher compared to that of Ga vacancies, except for Sb-rich conditions. This suggests that the interstitials could play an important role in the Ga diffusion. However, in the experiments by Bracht *et al.*<sup>2,3</sup> the diffusion was attributed to vacancies. They based this conclusion on the similarity of their results to the data by Mathiot and Edelin.<sup>29</sup> Mathiot and Edelin attributed the In impurity diffusion to vacancies, and observed an increased diffusion for Sb-rich conditions. In accordance with this idea, our data for the  $V_{\text{Ga}}$  concentration indeed shows an increase when moving towards Sb-rich conditions (Fig. 1). Nevertheless, it seems that the effect of the Ga interstitials should be analyzed more closely. For the Sb defects, our results show a larger concentration for the vacancies. In contrast, the experimental arguments for the diffusion vehicle support the choice of  $\text{Sb}_i$  over  $V_{\text{Sb}}$ .<sup>3</sup>



The amphoteric transformation of  $V_{\text{Sb}}$  [see Eq. (9)] has been proposed as a model to explain the presence of Ga vacancies even in Ga-rich conditions.<sup>2,3</sup> As discussed above, the transformation is energetically favorable and the resulting complex is  $V_{\text{Ga}}\text{Ga}_{\text{Sb}}$ . For Ga-rich growth conditions at  $T=450^\circ\text{C}$  the Fermi level is at 0.15 eV (Fig. 2), which corresponds to the value  $\sim -0.3$  eV for the reaction energy. The reaction energy for the complex to dissociate decreases from 1.0 to 0.25 eV as the Fermi level is moved from the VBM to the CBM. For the same conditions as above the reaction energy for the dissociation is  $\sim 0.9$  eV. If separated, there is a Coulomb repulsion between the defects due to their negative charge states. Reaction (9) followed by the dissociation of the complex can be thus a mechanism to supply Ga vacancies and antisites and decrease the number of Sb vacancies. Moreover, Fig. 1 shows that the concentration of  $V_{\text{Ga}}\text{Ga}_{\text{Sb}}$  exceeds that of  $V_{\text{Ga}}$  as one moves toward Ga-rich conditions. Therefore, if Reaction (9) and the subsequent dissociation are assumed to be effective, the  $V_{\text{Ga}}$  concentration levels off as one moves toward Ga-rich conditions.

The recombination of Sb interstitials and Ga vacancies is a reaction which has been proposed to explain the loss of Sb interstitials:<sup>2,3</sup>



To the left, this reaction is exothermic, by 3.0–3.4 eV depending on the Fermi level position, and further driven by the Coulomb attraction of the right-hand side defects. The right-hand-side defects were calculated in their well-separated configurations. We studied the recombination in more detail in the neutral charge state. We placed  $\text{Sb}_i$  at two tetrahedral positions close to the vacancy: one to a next-nearest-neighbor interstitial position  $T_a$  and the other to a nearest-neighbor position  $T_c$  (i.e., next to the vacancy). In the first case the system relaxed to the  $\text{Sb}_{\text{Ga}}$  antisite configuration without an energy barrier and in the second case to the close-lying metastable  $V_{\text{Ga}}\text{Sb}_i$  configuration also without a barrier. Reaction (12) could thus suppress the concentration of Sb interstitials in the presence of Ga vacancies. It should be noted that the native Sb interstitial concentration is in any case very low. However, the reaction may be important in the diffusion experiments that are performed in Sb-rich ambient conditions.

### C. Ga- and Sb-rich ambient conditions

In the experiment by Bracht *et al.*<sup>2,3</sup> diffusion measurements were performed for both Ga- and Sb-rich ambient conditions with the temperature varying between 571 and 708 °C.<sup>2,3</sup> The as-grown sample was considered to belong to the Ga-rich branch of the phase diagram. It was considered that the Sb-rich ambient did not significantly affect the sample composition during the Ga diffusion experiments. In contrast, due to the long diffusion times the Sb diffusion experiments performed under Sb-rich ambient conditions were considered to change the sample composition to correspond to Sb-rich growth conditions.<sup>3</sup> The main observations of these experiments were that the diffusion coefficient for

Ga is identical under Sb- and Ga-rich ambient conditions, and that there is a lack of significant diffusion of Sb under Ga-rich conditions.

On the basis of our data, two explanations can be given for the fact that the diffusion coefficient for Ga is identical under Sb- and Ga-rich ambient conditions.<sup>2,3</sup> First, we assume that the surface conditions do not affect the diffusion in any significant way. In this case the residual concentrations of the native defect  $V_{\text{Ga}}$  or  $\text{Ga}_i$  would be responsible for the diffusion. For the Ga-rich limit the concentrations are  $\sim 10^9$  and  $\sim 10^{17} \text{ cm}^{-3}$ , respectively. In the second explanation we take into account the surface conditions and assume that the Ga diffusion is mediated by Ga vacancies only. Under Sb-rich ambient conditions there is a surface supply of  $V_{\text{Ga}}$ , which thus directly mediates the diffusion. Under Ga-rich ambient conditions the Sb vacancy, supplied from the surface, undergoes the transition described by Eq. (9). If the complex  $V_{\text{Ga}}\text{Ga}_{\text{Sb}}$  is further dissociated, this means an effective supply of  $V_{\text{Ga}}$ . If the surface supply of the  $\text{Ga}_i$  defect would be responsible for Ga diffusion, the different surface conditions should produce differing diffusion coefficients. Although the first explanation is more appealing due to its simplicity, further experiments or kinetic calculations for the defect profiles are required to decide between the two hypotheses.

The other experimental finding was the lack of significant diffusion of Sb under Ga-rich conditions.<sup>2,3</sup> For Ga-rich conditions the concentrations of Sb vacancies and interstitials in the as-grown material are very low,  $\sim 10^9$  and  $\sim 0 \text{ cm}^{-3}$ , respectively. Furthermore, under Ga ambient conditions the surface does not supply defects that could mediate diffusion. For the Sb ambient conditions the picture is different. Due to the long diffusion times the material is actually assumed to reach a thermal equilibrium state which corresponds to Sb-rich growth conditions at  $\sim 700^\circ\text{C}$ .<sup>3</sup> We find that the concentrations of Sb vacancies and interstitials change now to  $\sim 10^{11}$  and  $\sim 10^6 \text{ cm}^{-3}$ , respectively, and there might also be a flow of Sb interstitials from the surface. Our results are thus in accordance with the idea that the increase of the  $\text{Sb}_i$  concentration switches on the weak Sb diffusion.

Bracht *et al.*<sup>3</sup> also reported preliminary studies on the effect of Zn doping on self-diffusion. For the Ga diffusion they found a strong intermixing of the Ga isotope layers, which indicates enhanced Ga diffusion. According to our results the *p*-type doping favors the formation of positively charged Ga self-interstitials, but has the opposite effect on the negatively charged Ga vacancies. We estimate that an extreme *p*-type doping would lower the formation energy of the Ga defect by  $\sim 0.1$ – $0.3$  eV (at 450 °C) for stoichiometric or Ga-rich growth conditions thus increasing its concentration. The increased diffusion via the  $\text{Ga}_i$  defect would be in contradiction with the vacancy model. For the Sb defects the formation energies of both vacancies and interstitials would decrease, but their concentration would still be small compared to that of Ga vacancies and interstitials. This would explain the fact that the Sb diffusion could not be resolved in the doped samples.



## V. CONCLUSIONS

We have made a comprehensive study of structures, formation energies, energy levels, and concentrations of native defects in undoped GaSb. The native defects show similarity in atomic and electronic structures with those in GaAs. A metastable state is found for the anion antisite  $\text{Sb}_{\text{Ga}}$ . An important difference compared to GaAs is that in GaSb the anion antisite  $\text{Sb}_{\text{Ga}}$  does not have ionization levels deep in the band gap, whereas in GaAs the ionization levels of the  $\text{As}_{\text{Ga}}$  antisite cause the semi-insulating character of the as-grown material. The as-grown GaSb is predicted, in accordance with experiments, to be  $p$  type under different growth conditions. The reason for this character is the  $\text{Ga}_{\text{Sb}}$  antisite, which acts as the dominant residual acceptor.

The concentrations of the relevant defects estimated for typical experimental conditions are used to discuss the observed highly asymmetric self-diffusion of Ga and Sb in GaSb, i.e., the phenomenon that the diffusion of Ga is several orders in magnitude faster than that of Sb. We conclude that the significant concentration differences between the defects in the different sublattices explain the experimental finding. However, for the Ga diffusion, in contrast to the vacancy model by Bracht *et al.*,<sup>2,3</sup> our data suggests that the formation of Ga interstitials may play a role. In the case of the Sb diffusion, a high temperature and Sb-rich ambient conditions are found to increase the concentration of Sb interstitials and thereby the Sb self-diffusion. In order to resolve the actual atomistic diffusion mechanism (vacancy or interstitial) for both elements, it would be necessary to perform simulations for the diffusivities.

## ACKNOWLEDGMENTS

We acknowledge the generous computer resources from the Center for Scientific Computing, Espoo, Finland. This research has been supported by the Academy of Finland through its Centers of Excellence Program (2000–2005).

- <sup>1</sup>P. S. Dutta, H. L. Bhat, and V. Kumar, *J. Appl. Phys.* **81**, 5821 (1997).
- <sup>2</sup>H. Bracht, S. P. Nicols, W. Walukiewicz, J. P. Silveira, F. Briones, and E. E. Haller, *Nature (London)* **408**, 69 (2000).
- <sup>3</sup>H. Bracht, S. P. Nicols, E. E. Haller, J. P. Silveira, and F. Briones, *J. Appl. Phys.* **89**, 5393 (2001).
- <sup>4</sup>C. Anayama, T. Tanahashi, H. Kuwatsuka, S. Nishiyama, S. Isozumi, and K. Nakajima, *Appl. Phys. Lett.* **56**, 239 (1990).
- <sup>5</sup>K. F. Longenbach and W. I. Wang, *Appl. Phys. Lett.* **59**, 2427 (1991).
- <sup>6</sup>U. Scherz and M. Scheffler, in *Imperfections in III/V Materials*, edited by R. Weber (Academic, New York, 1993), p. 3.
- <sup>7</sup>M. J. Caldas, J. Dabrowski, A. Fazzio, and M. Scheffler, *Phys. Rev. Lett.* **65**, 2046 (1990).
- <sup>8</sup>W. Kühn, R. Strehlow, and M. Hanke, *Phys. Status Solidi B* **141**, 541 (1987).
- <sup>9</sup>H. Xu, *J. Appl. Phys.* **68**, 4077 (1990).
- <sup>10</sup>D. N. Talwar and C. S. Ting, *Phys. Rev. B* **25**, 2660 (1982).
- <sup>11</sup>M. J. Puska, *J. Phys.: Condens. Matter* **1**, 7347 (1989).
- <sup>12</sup>P. Hohenberg and W. Kohn, *Phys. Rev.* **136**, B864 (1964).
- <sup>13</sup>W. Kohn and L. J. Sham, *Phys. Rev.* **140**, A1133 (1965).
- <sup>14</sup>M. C. Payne, M. P. Teter, D. C. Allan, T. A. Arias, and J. D. Joannopoulos, *Rev. Mod. Phys.* **64**, 1045 (1992).
- <sup>15</sup>G. B. Bachelet, D. R. Hamann, and M. Schlüter, *Phys. Rev. B* **26**, 4199 (1982); D. R. Hamann, *ibid.* **40**, 2980 (1989).
- <sup>16</sup>N. Troullier and J. L. Martins, *Phys. Rev. B* **43**, 1993 (1991).
- <sup>17</sup>S. G. Louie, S. Froyen, and M. L. Cohen, *Phys. Rev. B* **26**, 1738 (1982).
- <sup>18</sup>G. Makov, R. Shah, and M. C. Payne, *Phys. Rev. B* **53**, 15513 (1996).
- <sup>19</sup>M. J. Puska, S. Pöykkö, M. Pesola, and R. M. Nieminen, *Phys. Rev. B* **58**, 1318 (1998).
- <sup>20</sup>S. B. Zhang and J. E. Northrup, *Phys. Rev. Lett.* **67**, 2339 (1991).
- <sup>21</sup>G. Makov and M. C. Payne, *Phys. Rev. B* **51**, 4014 (1995).
- <sup>22</sup>*Handbook of Chemistry and Physics*, 76th ed., edited by D. R. Lide (CRC Press, Boca Raton, 1995), p. 5-4.
- <sup>23</sup>Tilde in front of the symmetry symbol means that the ions are slightly, i.e., of the order of 3% of the bond length, moved from the symmetry positions given.
- <sup>24</sup>K. Laasonen, R. M. Nieminen, and M. J. Puska, *Phys. Rev. B* **45**, 4122 (1992).
- <sup>25</sup>G. A. Baraff and M. Schlüter, *Phys. Rev. Lett.* **55**, 1327 (1985).
- <sup>26</sup>J. Dabrowski and M. Scheffler, *Phys. Rev. B* **40**, 10391 (1989).
- <sup>27</sup>M.-C. Wu and C.-C. Chen, *J. Appl. Phys.* **72**, 4275 (1992).
- <sup>28</sup>M. Bockstedte and M. Scheffler, *Z. Phys. Chem. (Leipzig)* **200**, 195 (1997).
- <sup>29</sup>D. Mathiot and G. Edelin, *Philos. Mag. A* **41**, 447 (1980).